RESEARCH ARTICLE

Molecular Nutrition & Food Research
www.mnf-journal.com

The Ablation of Sensory Neurons Expressing the Nav1.8 Sodium Channel Improves Glucose Homeostasis and Amplifies the GLP-1 Signaling in Obese Female Mice

Marina Romaní-Pérez, Clara Bullich-Vilarrubias, Inmaculada López-Almela, and Yolanda Sanz*

Scope: Sensory neurons expressing the sodium channel Nav1.8 contain a repertoire of receptors for nutrient, hormonal, and inflammatory ligands. However, their function in key regulators of energy homeostasis control is not well understood and is completely unexplored in females.
Methods and results: Mice lacking neurons expressing the sodium channel Nav1.8 were generated using an ablation strategy based on cre recombinase-mediated expression of diphtheria toxin fragment A (DTA) (Nav1.8-cre/DTA mice) to investigate whether these neurons modulate body weight, food intake, gut hormone secretion, gastrointestinal transit, and glucose tolerance in response to nutrient challenges in a sex-dependent manner. Male Nav1.8-cre/DTA mice show resistance to gain weight in response to high-fat high-sugar diet (HFHSD), whereas females lacking Nav1.8+ neurons have improved oral glucose tolerance accompanied by higher insulin levels and attenuated glucagon secretion after an oral glucose load. Female Nav1.8-cre/DTA mice also show higher fasting and postprandial glucagon like peptide-1 (GLP-1) levels with an increased number of GLP-1-positive cells. Finally, ablation of Nav1.8-expressing neurons accelerates the gastrointestinal transit in female mice under HFHSD.
Conclusion: This data demonstrates sex-dependent differences in the Nav1.8-mediated regulation of energy metabolism, and provides new insights that may help in the design of sex-specific neuromodulation therapies for metabolic disorders induced by diets rich in fats and simple sugars.

1. Introduction

Obesity has reached epidemic proportions globally, and has myriad associated comorbidities, such as type 2 diabetes (T2D), which increase morbidity and mortality. Despite the great strides made to understand the key factors controlling energy homeostasis, efforts are still needed to reduce the prevalence of obesity, including new therapies.

The gut is now considered a key target in the development of therapies for obesity. Gastrointestinal endocrine and neural sensory pathways play an important role in nutrient sensing to further control energy homeostasis. The major players of these pathways are enteroendocrine cells (EECs) and vagal afferents. Nutrient sensing G protein-coupled receptors (GCPRs) on EECs are activated by dietary molecules and trigger the secretion of gut hormones that control many physiological functions via endocrine paths such as gut motility, appetite and glucose metabolism, among others. This activation also stimulates vagal afferents to rapidly transmit nutrient sensing to the brain.[1,2]

Bariatric surgery, the most effective treatment for weight loss and glycemic control,[3,4] induces its benefits by enhancing the postprandial secretion of gut hormones in the distal gut, owing to the higher availability of unabsorbed nutrients in this region.[5] Bariatric surgery mimetic approaches for T2D include non-invasive gut-peptide strategies or those that favor gut hormone secretion.[6,7] Analogues of the gut hormone glucagon like peptide-1 (GLP-1) are established glucose-lowering agents for T2D,[8] and the clinical efficacy of agonists of the chemoreceptors that induce GLP-1 secretion are under intense investigation.[6]

In a different approach, neuromodulation therapies including either stimulation (vagus nerve stimulation therapy [VNS]) or inhibition (vagal nerve blocking therapy [VBLOC]) of the vagal nerve by low- or high-frequency currents, respectively, induce weight loss and improve obesity-related metabolic parameters.[9–11] Nevertheless, the mechanisms responsible for these benefits, and whether afferent or efferent tone are preferentially involved, are enigmatic.[10]

M. Romaní-Pérez, C. Bullich-Vilarrubias, I. López-Almela[+], Y. Sanz
Institute of Agrochemistry and Food Technology
Spanish National Research Council (IATA-CSIC)
Valencia, Spain
E-mail: marina.romani@iata.csic.es

The ORCID identification number(s) for the author(s) of this article can be found under https://doi.org/10.1002/mnfr.202300474

[+]Present address: Research Group Intracellular Pathogens: Biology and Infection, Department of Animal Production and Health, Veterinary Public Health and Food Science and Technology, Faculty of Veterinary Medicine, Cardenal Herrera-CEU University, Valencia, Spain

DOI: 10.1002/mnfr.202300474

Currently, the therapeutic potential of the modulation of sensory neurons from the peripheral nervous system remains understudied, as its diverse molecular specialization makes it difficult to investigate the role of specific neuronal populations.[11]

Genetic tools to target neurons expressing specific molecular markers are now reshaping our understanding of the functions of afferent neurons on energy homeostasis control. For instance, Cre-LoxP-based experiments conducted in mice point out new functions of sensory neurons expressing the sodium channel Nav1.8, hitherto characterized as spinal neurons mediating pain sensation.[12] More specifically, the vagal origin of Nav1.8+ neurons innervating the gastrointestinal tract has been demonstrated[13,14] highlighting their function driving visceral information to the brain and so, controlling energy balance. Investigations on this topic demonstrated that these neurons are dispensable for the control of body weight, food intake, or energy expenditure.[15] In contrast, another study revealed that, although Nav1.8+ neurons are not involved in weight gain due to high-fat dietary intake, they are necessary for maintaining fat stores while contributing to metabolic balance.[16] In addition, characterization of GCPR gene expression profiles points to a role for these neurons in mediating gut-to-brain communication triggered by gut-derived molecules such as hormones or immunomodulatory lipids.[17] In this regard, it is not yet known whether Nav1.8+ neurons are needed for gastrointestinal functions that influence postprandial control of energy metabolism and whether they exhibit sex-dependent effects. This research would help advance more precise neuromodulation-based strategies for obesity by targeting a specific neuronal population in the afferent arm of the peripheral nervous system. Using a murine ablation model lacking Nav1.8-expressing neurons we have identified sex-dependent metabolic functions of these neurons. Specifically, in females, we have unraveled intestinal factors through which Nav1.8+ neurons regulate energy homeostasis.

2. Results

2.1. Lack of Nav1.8-Expressing Neurons Has a Sex-Dependent Effect on Body Weight Gain, Fasting Induced Refeeding, and Glucose Tolerance in Mice Fed a High-Fat High-Sugar Diet

Since vagal afferents, rather than spinal neurons, are involved in nutrient sensing to further control energy homeostasis, Nav1.8 gene expression was explored in nodose ganglia. Mice expressing Cre, hereinafter referred to as mice lacking Nav1.8+ neurons or mice lacking the sodium channel Nav1.8 (Nav1.8-cre/DTA) mice, had almost undetectable *Scn10a* mRNA levels (coding for NAV1.8), indicating effective ablation of Nav1.8+ neurons in the offspring (Supporting Information Figure S1b).

We examined the vulnerability to gain weight in response to high-fat high-sugar diet (HFHSD)-feeding in Nav1.8-cre/DTA mice and potential interactions between sex and the genotype. The effects on body weight were examined after 5 weeks of HFHSD-feeding, before conducting other functional tests (between week 6 and 11) to avoid the influence of the stress associated with these tests.

An interaction between the group and the week of control diet (CD)/HFHSD-feeding was identified in the body weight of both, females and males (**Figure 1A**), indicating that this parameter varies differentially over 5 weeks of dietary intervention. As expected, at least from week 4, HFHSD-feeding increased the body weight of female and male control mice compared with controls fed CD (Figure 1A). Furthermore, under HFHSD and only in males, Nav1.8-cre/DTA mice showed reduced body weight than their control littermates (Figure 1A). Overall, 5 weeks of HFHSD-feeding increased the body weight gain of both, female and males since a main diet effect was identified in both sexes (Figure 1B). A genotype effect was also detected, but only on the body weight gain of male mice, supporting that loss of Nav1.8-expressing neurons induces obesity resistance in males (Figure 1B).

Ad libitum food intake was not markedly affected by the genotype in female and male mice (Supporting Information Figure S2a). By contrast, analysis of 2-h food intake after fasting revealed a diet effect only in females irrespective the genotype, with reduced food intake in the refeeding period in mice fed HFHSD (Figure 1C, left graph). An interaction between diet and the genotype was identified in males (Figure 1C, right graph). Post-hoc analysis revealed that HFHSD-fed Nav1.8-cre/DTA male mice had a higher food intake after fasting than controls fed the obesogenic diet or Nav1.8-cre/DTA mice fed CD (Figure 1C, right graph). Body weight gain after the refeeding was lower in HFHSD fed female and male mice irrespective of the genotype compared with CD-fed groups (Figure 1D). Food efficiency was also affected by the diet and the genotype in female and male mice (Figure 1E). Specifically, we found an interaction between diet and genotype in females, whereby food efficiency was lower in HFHSD-fed control mice than in CD-fed mice, with no effects in Nav1.8-cre/DTA mice (Figure 1E, left graph). In males, the diet and the genotype impacted food efficiency, and both variables showed a trend for interaction ($p = 0.08$) (Figure 1E, right graph). Analysis restricted to HFHSD-fed mice indicated that food efficiency showed a trend to be lower in Nav1.8-cre/DTA mice than in control littermates (Student's *t*-test, Cre^- HFHSD versus Cre^+ HFHSD, $p = 0.09$).

In response to an obesogenic diet, we explored whether the loss of Nav1.8+ neurons affected weight gain and food efficiency differently in males or females by identifying sex and genotype interactions on these parameters (datasets from Figure 1B,E). First, we observed high inter-individual variability in the body weight gain of Nav1.8-Cre/DTA male mice fed HFHSD (see extending whiskers in Figure 1B indicating variability outside the upper and lower quartiles), supporting that loss of Nav1.8+ neurons may induce diverse responses to HFHSD-feeding, as already evidenced by others.[15] Using a protocol similar to that used in previous rodent studies,[20,27,28] we employed quartile distribution to identify individual vulnerability to diet-induced obesity allowing a more accurate exploration of sex-genotype interactions taking into account the variability of response to an obesogenic diet. Thus, each HFHSD-fed group was subdivided into weight-gaining or obesity-prone mice, whose weight gain belonged to the first quartile (Q1); non- weight-gaining or obesity resistant mice, belonging to Q2 and Q3; and weight-losing or cachectic mice, belonging to Q4 (Figure 1F).

No sex-associated differences in the quartile distribution of weight gain data were found irrespective of the genotype (males: $\chi^2 = 0.564$, $p = 0.754$ or females: $\chi^2 = 0.012$, $p = 0.994$). We found an interaction between genotype and sex in the weight gains distributed in Q2/Q3 and in Q4 (Figure 1F). Specifically, in

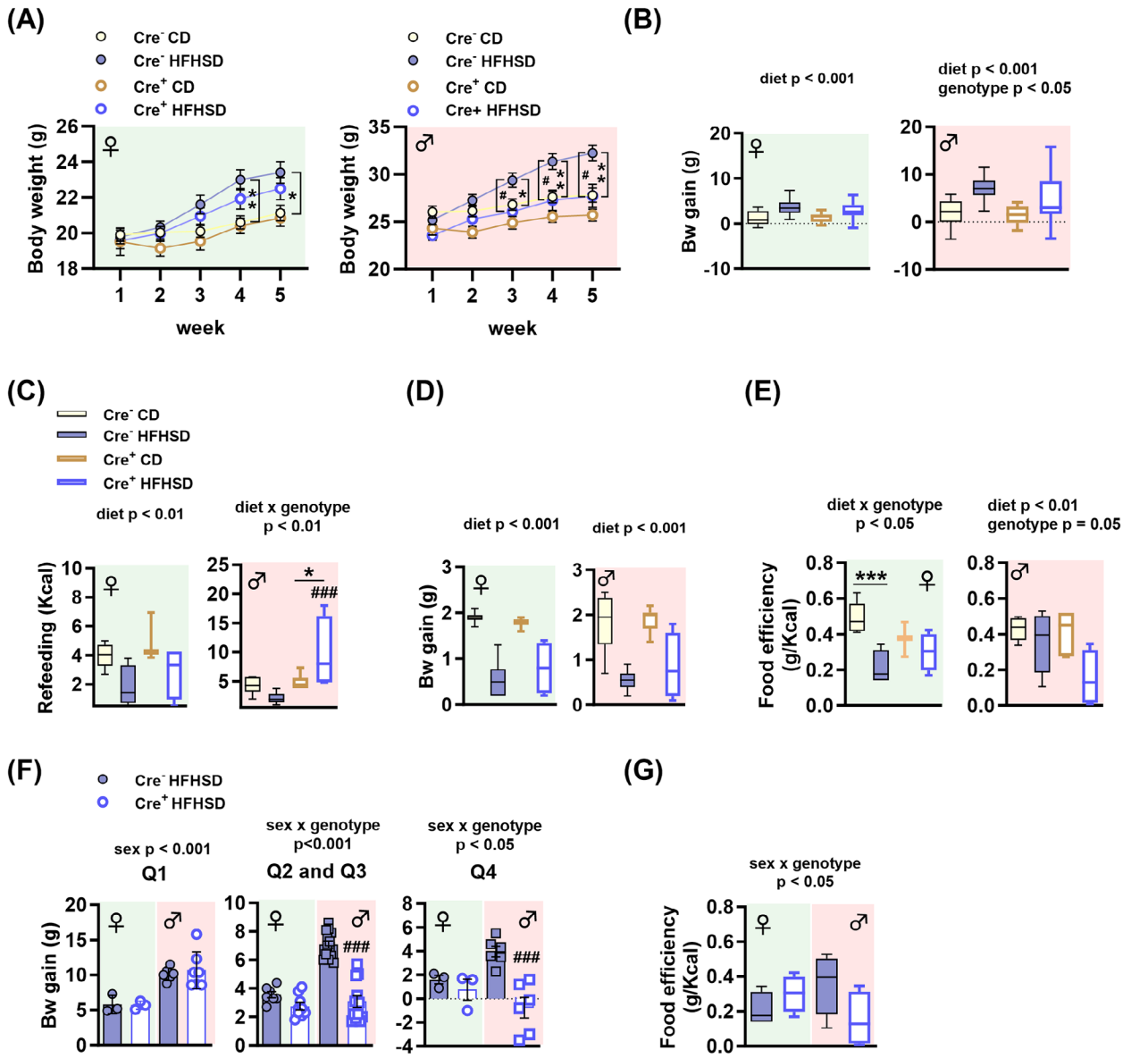

Figure 1. Ablation of neurons expressing the sodium channel Nav1.8 has sex-dependent effects on body weight under an obesogenic diet. In female and male controls and mice lacking neurons expressing the sodium channel Nav1.8 (Cre^{-}/Cre^{+}) fed either control or high-fat high-sugar diet (CD/HFHSD), we measured: A) Body weight (Bw) follow-up and B) Bw gain of females and males in response to 5 weeks of CD or HFHSD. C) Food intake (kcal) during refeeding after fasting in the dark phase. D) Bw gain after refeeding. E) Food efficiency. F) Comparisons of the Bw gain separated into quartiles (Q) of female and male mice fed HFHSD. G) Comparison of the food efficiency of female or male mice fed HFHSD. Data show the mean ± standard error of the mean (SEM) or the median, the interquartile range and the minimum and maximum values (whiskers). (A, B, F) Data from three cohorts, no significant cohort effect was observed. Female Cre^{-} CD/HFHSD, $n = 20$; female Cre^{+} CD, $n = 8$; female Cre^{+} HFHSD, $n = 15$; male Cre^{-} CD/HFHSD, $n = 23/25$; male Cre^{+} CD, $n = 13$, and Cre^{+} HFHSD, $n = 27$. (C–E, G) Data from 1 cohort. Female Cre^{-} CD/HFHSD, $n = 6$; female Cre^{+} CD/HFHSD, $n = 4$; male Cre^{-} CD/HFHSD, and $n = 8$ and male Cre^{+} CD/HFHSD, $n = 7/5$. HFHSD-data of (B) are also represented in (F). HFHSD-data of (E) are also represented in (G). Two-way analysis of variance (ANOVA) followed by Tukey's post-hoc test when significant interactions were detected. Main effects and interactions are indicated on top of the graphs. $^{*}p < 0.05$ and *** $p < 0.001$ versus CD-fed mice with the same genotype. $^{\#\#\#}$ $p < 0.001$ versus HFHSD-fed mice with different genotypes.

response to 5 weeks of HFHSD-feeding, male Nav1.8-Cre/DTA mice, but not females, gained less weight than their control littermates, occasionally showing weight loss in the case of male mice distributed in Q4 (Figure 1F). No interaction was found in mice from Q1 (Figure 1F). In addition, a combinatorial effect between sex and genotype was found in food efficiency, with a tendency to show reduced food efficiency in male mice lacking Nav1.8+ neurons compared to control littermates ($p = 0.09$), not shown in females (Figure 1G).

Genotype- and sex-related effects on fat depots were also examined. First, we examined fat distribution, calculated as the percentage of individual fat pad mass (gonadal white adipose tissue

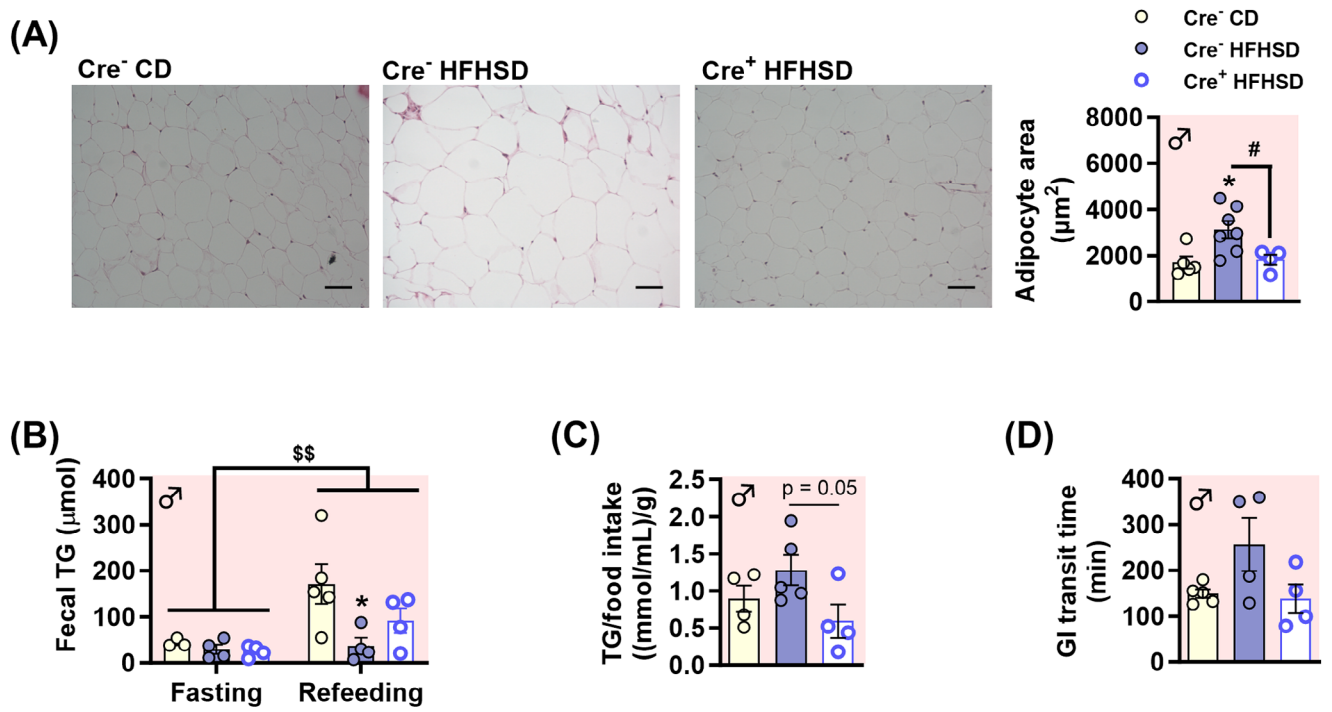

Figure 2. Loss of Nav1.8+ neurons limits fat storage in the gonadal adipose tissue in male mice fed high-fat high-sugar diet. In male controls (Cre^-) fed control diet (CD) or high-fat high-sugar diet (HFHSD) and mice lacking Nav1.8+ neurons fed HFHSD, we measured: A) Adipocytes area in the gonadal white adipose tissue at the end of the experiment. B) Total triglyceride (TG) levels excreted in feces after 12 h of overnight fasting, preceding the gastrointestinal transit time trial and during the trial (6 h of refeeding) after 8 weeks of CD or HFHSD-feeding. C) TG in plasma after 2 h of refeeding at week 7 of CD or HFHSD-feeding. D) Time required for orally administered carmine red to appear in feces (gastrointestinal [GI] transit time) after 8 weeks of CD or HFHSD-feeding. Data are shown as the mean ± standard error of the mean (SEM). Cre^- CD, $n = 5$, Cre^- HFHSD, $n = 7$–5, and Cre^+ HFHSD, $n = 4$. (A, C, D) One-way analysis of variance (ANOVA) followed by Tukey's post-hoc test. (B) Two-way ANOVA. $^*p < 0.05$ versus CD-fed control mice (Cre^- CD). $^{\#}$ $p < 0.05$ versus HFHSD-fed mice with different genotypes. $^{\$\$}$ $p < 0.01$ main effect of prandial condition (fasting versus refeeding).

[gWAT] or inguinal white adipose tissue [iWAT]) relative to total fat pad mass (iWAT plus gWAT). As indicated by a main effect of fat type, there was a greater contribution of gWAT to total fat depots in both female and male mice (Supporting Information Figure S2b). In addition, the analysis of the combinatory effects of genotype and sex revealed that fat distribution was affected by sex but not by the genotype (Supporting Information Figure S2c). Indeed, regardless the genotype, a main effect of sex was identified on the distribution of gWAT and iWAT, indicating higher gonadal fat pads in male than in female and higher iWAT in female than in male (Supporting Information Figure S2c).

Despite fat distribution remained unaffected by the genotype, we identified that, only in males, the loss of Nav1.8-expressing neurons had an impact on gWAT weight. Indeed, after 11 weeks of HFHSD-feeding, Nav1.8-cre/DTA female mice showed the same gWAT weight as controls (controls: 0.67 ± 0.12 g versus Nav1.8-cre/DTA: 0.55 ± 0.20 g, $p = 0.60$), while Nav1.8-Cre/DTA male mice (from Q2 and Q3) had reduced gWAT (controls: 1.70 ± 0.20 g versus Nav1.8-cre/DTA: 0.69 ± 0.27 g, $p = 0.04$). The lower gWAT in male mice lacking Nav1.8+ neurons was further supported by the smaller adipocyte size compared with HFHSD-fed controls, reaching values similar to CD-fed control mice (**Figure** 2A), suggesting a reduced storage of lipids in adipocytes.

To unravel how loss of Nav1.8-expressing neurons limits fat depots in males, we examined in these mice the influence of the genotype on dietary lipids excretion and absorption by measuring triglycerides in feces and plasma after a meal and by exploring gastrointestinal transit time. A main effect of the prandial condition (fasting/refeeding) on fecal triglycerides levels was identified, with higher triglycerides levels in feces after 6 h of refeeding compared with 12 h of fasting (Figure 2B). After fasting, fecal triglycerides levels did not show significant differences between groups, but total excreted triglycerides during 6 h of refeeding were lower in HFHSD-fed control male mice than in equivalent Nav1.8-Cre/DTA mice, which had levels similar to those of CD-fed control mice (Figure 2B). Furthermore, under HFHSD, Nav1.8-cre/DTA male mice showed reduced postprandial triglycerides levels in plasma than controls (Figure 2C). The gastrointestinal transit time, which may impact on the intestinal excretion and absorption of lipids, was not significantly affected by the diet or the genotype (Figure 2D).

We then explored the impact of Nav1.8+ neurons ablation on the control of glucose homeostasis. In female mice, an interaction between the genotype and the diet was identified in fasting glycemia (**Figure** 3A). Further post-hoc analysis indicated that HFHSD increased the basal glucose levels compared with CD in Nav1.8-cre/DTA female mice (Figure 3A, left graph). In male mice, neither main effects nor interactions between the genotype and the diet were detected (Figure 3A, right graph). The analysis of the oral glucose tolerance test (OGTT) indicated a main effect of the genotype in female mice (Figure 3B) but not in

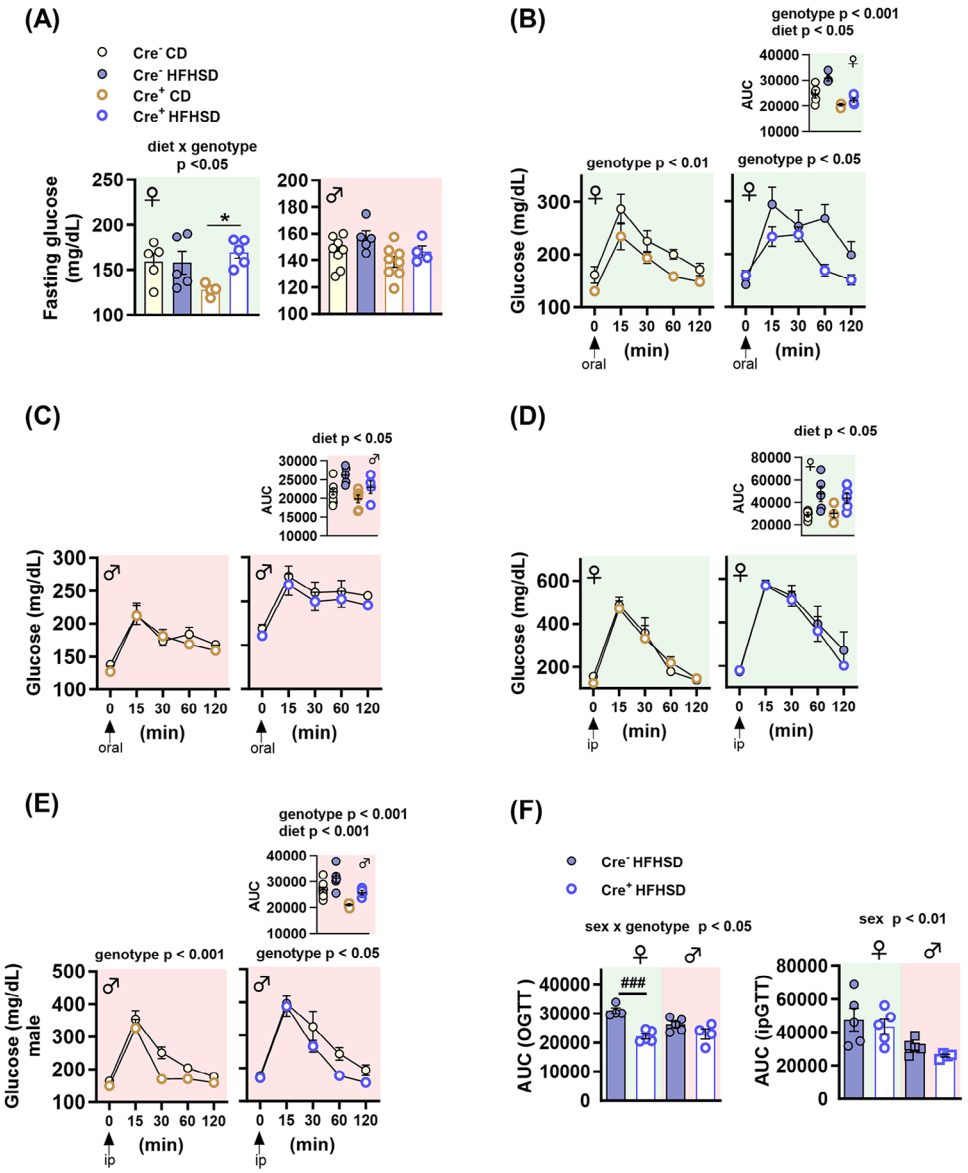

Figure 3. Deficiency of Nav1.8+ neurons improves oral glucose tolerance in females and intraperitoneal glucose tolerance in males. In female or male controls and mice lacking Nav1.8+ neurons (Cre^{-}/Cre^{+}) fed either control or high-fat high-sugar diet (CD/HFHSD) for 10 weeks, we measured: A) Fasting glucose levels in plasma of female and male mice. B, C) Oral glucose tolerance test (OGTT) and the area under the curve (AUC). D, E) Intraperitoneal glucose tolerance test (ipGTT) and AUC. F) Comparison of the AUC of the OGTT between females and males (Cre^{-}/Cre^{+}) fed HFHSD (left) and comparison of the AUC of the ipGTT between females and males (Cre^{-}/Cre^{+}) fed HFHSD (right). Data are shown as the mean ± standard error of the mean (SEM). Female mice, $n = 5$ per group and male mice, $n = 5$–8 per group. HFHSD-data of AUC of (B-E) are also represented in (F). Two-way analysis of variance (ANOVA) followed by Tukey's post-hoc test when significant interactions were detected. Main effects and interactions are indicated on top of the graphs. $^{*}p < 0.05$ Cre^{+} fed CD versus HFHSD. $^{\#\#\#}p < 0.001$ versus HFHSD-fed mice with different genotypes.

males (Figure 3C) indicating that the whole-body glucose clearance was more efficient in female Nav1.8-Cre/DTA mice than in their control littermates after an oral glucose load under either CD or HFHSD (Figure 3B). When glucose was intraperitoneally (ip) administered to mice, the whole-body glucose clearance was improved in male Nav1.8-Cre/DTA mice (Figure 3E) but not in females (Figure 3D). A diet effect was found in the area under the curve (AUC) of the OGTT and intraperitoneal glucose tolerance test (ipGTT) in female and male mice (Figure 3B–E), confirming that, irrespective the genotype, HFHSD impairs glucose tolerance. We found an interaction between sex and genotype for the AUC of the OGTT in mice fed HFHSD with more robust glycemia reduction in female Nav1.8-Cre/DTA mice than in males as indicated the post-hoc test (Figure 3F, left graph), although no combinatory effects were observed for the AUC of the ipGTT (Figure 3F, right graph).

Taken together, our findings support sex-dependent metabolic functions of Nav1.8+ neurons in which, in response to an

obesogenic diet, Nav1.8+ silencing attenuates weight gain and adiposity in males but not in females and improves oral glucose tolerance in females but not in males.

2.2. Loss of Nav1.8-Expressing Neurons Increases the Plasma Levels of Total GLP-1 and Insulin in Female Mice Fed a High-Fat High-Sugar Diet

Longer term analysis of health status of mice (9 weeks of HFHSD-feeding) revealed that female Nav1.8-cre/DTA mice showed optimal health and welfare in response to HFHSD-feeding, whereas male Nav1.8-cre/DTA showed sickness behavioral responses to HFHSD. Indeed, in response to 9 weeks of HFHSD-feeding, female mice lacking Nav1.8+ neurons gained the same weight as controls (Supporting Information Figure S2d,e). In contrast, some Nav1.8-cre/DTA male mice showed body weight loss through the HFHSD intervention (Supporting Information Figure S2f, right graph) occasionally reaching almost 8% weight loss from their initial body weight (Supporting Information Figure S2g, right graph). Those Nav1.8-cre/DTA male mice that lost weight under HFHSD showed ulcerative dermatitis (data not shown) and finally died. Indeed, only the 50% of Nav1.8-cre/DTA male mice survived after 9 weeks of HFHSD-feeding (Supporting Information Figure S2h, right graph). By contrast, the obesogenic diet did not affect the survival of Nav1.8-cre/DTA female mice (Supporting Information Figure S2h, left graph). To note, the experiments in male mice (Figures 2 and 3) were conducted in mice that did not show sickness behavior (mice which body weight gain belonged to Q2 and Q3).

As Nav1.8+ neurons ablation did not affect female health, the exploration of the effects of long-term exposure to HFHSD were restricted to female mice.

On the basis that Nav1.8+ neurons mediate neuroimmune pathways in mucosa layers,[23,24] we began to explore the intestinal mechanisms underlying the glucoregulatory benefits of Nav1.8+ neurons in diet-induced obese female mice by first examining intestinal immunity, which imbalance may disturb glucose homeostasis.[25]

In the lamina propria of the small intestine, Nav1.8-cre/DTA mice had higher levels of type 1 and type 2 macrophages (M1 and M2) and regulatory T cells (Treg) (Supporting Information Figure S3a–c). In addition, the absence of Nav1.8+ neurons conferred protection against the spleen enlargement showed in HFHSD-fed control mice (Supporting Information Figure S3d), increased the splenic levels of memory CD4+ T cells (Supporting Information Figure S3e) and tended to reduce the levels of effector CD4+ T cells (Supporting Information Figure S3f).

As alternative intestinal mechanisms potentially involved in the glucoregulatory benefits of the Nav1.8+ neurons depletion, we also investigated glucose absorption and incretin hormone (GLP-1 and gastric inhibitory polypeptide [GIP]) secretion together with the hormones regulated by those incretins (insulin and glucagon) in response to an oral glucose challenge. Intestinal glucose uptake was faster in Nav1.8-cre/DTA mice than in control mice, as indicated by the enhanced early appearance of glucose in the bloodstream immediately after an oral glucose challenge (5 min post-glucose) (**Figure** 4A), despite their lower glycemia in the OGTT from minute 15 onwards, which refers to glucose clearance (Figure 3A). No changes were identified in the gene expression of the glucose transporters *Slc2a2* (coding for GLUT2) (Supporting Information Figure S3g) and *Slc5a1* (coding for sodium-glucose transport protein 1, [SGLT1]) (Supporting Information Figure S3h) in the proximal small intestine, or in the small intestine length (Supporting Information Figure S3i).

Compared with CD-fed controls, HFHSD-fed control mice had lower total GLP-1 levels in plasma but higher GIP during fasting, and showed increased GIP and glucagon levels after an oral glucose load (Figure 4B). Nav1.8-cre/DTA mice had higher insulin levels than CD-fed mice both during fasting and after glucose challenge, with similar levels of total GLP-1, GIP, and glucagon (Figure 4B). Combinatorial effects of the genotype and the prandial condition on hormone levels were investigated in HFHSD-groups. We found an interaction between genotype and prandial condition for total GLP-1 (Figure 4B), with post-hoc analysis indicating that total GLP-1 levels were higher in Nav1.8-cre/DTA mice than in control mice during fasting but not after the oral glucose load (Figure 4B). Furthermore, independently of the prandial condition, the absence of Nav1.8-expressing neurons prevented the increase in GIP levels induced by HFHSD-feeding (Figure 4B). In addition, a main effect of the genotype was also detected on insulin indicating that Nav1.8-cre/DTA mice showed increased levels of this hormone in both conditions (fasting and after an oral glucose load) compared with HFHSD-fed control mice (Figure 4B). At the end of the experiment, total GLP-1 levels in plasma were measured in response to an oral load of the mixed-nutrient solution, Ensure®. No changes were observed 15 min after Ensure® (Figure 4C), but after 90 min, a main effect of the diet and the genotype were identified on the total GLP-1 levels in plasma (Figure 4D). These main effects indicated that HFHSD-feeding reduced total GLP-1 whatever the genotype, and that the ablation of Nav1.8+ neurons increased its levels compared with control littermates irrespective of the diet (Figure 4D).

The loss of Nav1.8+ neurons might impact gut-to-brain nutrient sensing and, consequently, the central control of glucose homeostasis. Analysis of the expression of key hypothalamic genes for energy homeostasis control evidenced no major changes associated with the genotype. Proopiomelancortin (*Pomc*) and cocaine- and amphetamine-regulated transcript (*Cart*) were unchanged whatever the group, whereas aguti-related peptide (*Agrp*) and neuropeptide Y (*Npy*) transcripts were lower in control and Nav1.8-cre/DTA mice fed HFHSD than in CD-fed control mice (Supporting Information Figure S3j), reflecting that Nav1.8-cre/DTA mice downregulated orexigenic neuropeptides to counteract the excess of high-energy dense food as did HFHSD-fed control mice.

2.3. Loss of Nav1.8+ Neurons Increases the Density of Intestinal Cells Expressing GLP-1 in Female Mice Fed a High-Fat High-Sugar Diet

Gene expression analysis of markers of stem cells, proliferation, and L-cell differentiation after oral Ensure® challenge revealed that the loss of Nav1.8+ neurons prevented the higher ileal expression of *Ki67* induced by HFHSD-feeding and enhanced

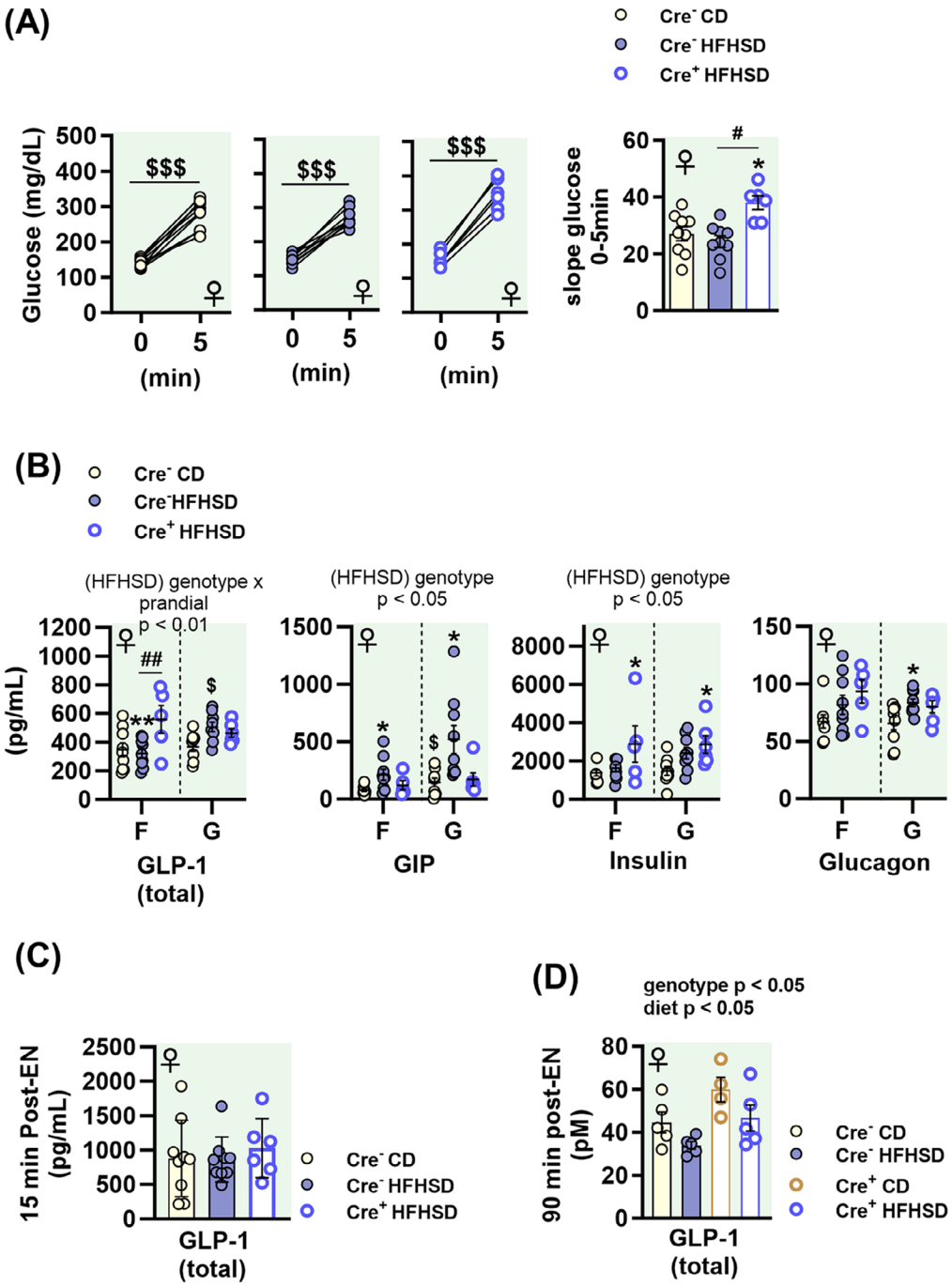

Figure 4. Deficiency of Nav1.8+ neurons increases plasma levels of total glucagon like peptide-1 (GLP-1) and insulin in female mice fed high-fat high-sugar diet. In female controls (Cre⁻) fed control or high-fat high-sugar diet (CD or HFHSD, respectively) and mice lacking Nav1.8+ neurons (Cre⁺) fed HFHSD, we measured: A) Fasting glycemia and 5 min after an oral glucose load and the slope between these two points, indicating glucose intestinal uptake, after 7 weeks of CD- or HFHSD-feeding. B) Plasma levels of total (GLP-1), GIP, insulin, and glucagon, in fasting (F) and 15 min after an oral glucose load (G), after 7 weeks of CD- or HFHSD-feeding. C) Plasma levels of total GLP-1 15 min after the oral administration Ensure® (EN). D) Total GLP-1 levels in plasma 90 min after administering Ensure®. Data are shown as the mean ± standard error of the mean (SEM) or paired individual values. Cre⁻ CD/HFHSD, $n = 5–9$, Cre⁺ CD = 4 and Cre⁺ HFHSD, $n = 5–6$. (A) Paired *t*-test; (slope data in A): one-way analysis of variance (ANOVA) followed by Tukey's post-hoc test. (B) (HFHSD data) and (D) two-way ANOVA followed by Tukey's post-hoc test when interactions were detected. Main effects and interactions are indicated on top of the graphs. (B) One-way ANOVA followed by Tukey's post-hoc test for comparisons with Cre⁻ CD group. $^{*}p < 0.05$ and $^{***}p < 0.001$ versus Cre⁻ CD-fed mice. $^{\#}p < 0.05$, $^{\#\#}p < 0.01$ comparisons between Cre⁻ and Cre⁺ fed HFHSD. $^{\$}p < 0.05$ and $^{\$\$\$}p < 0.001$ F versus G.

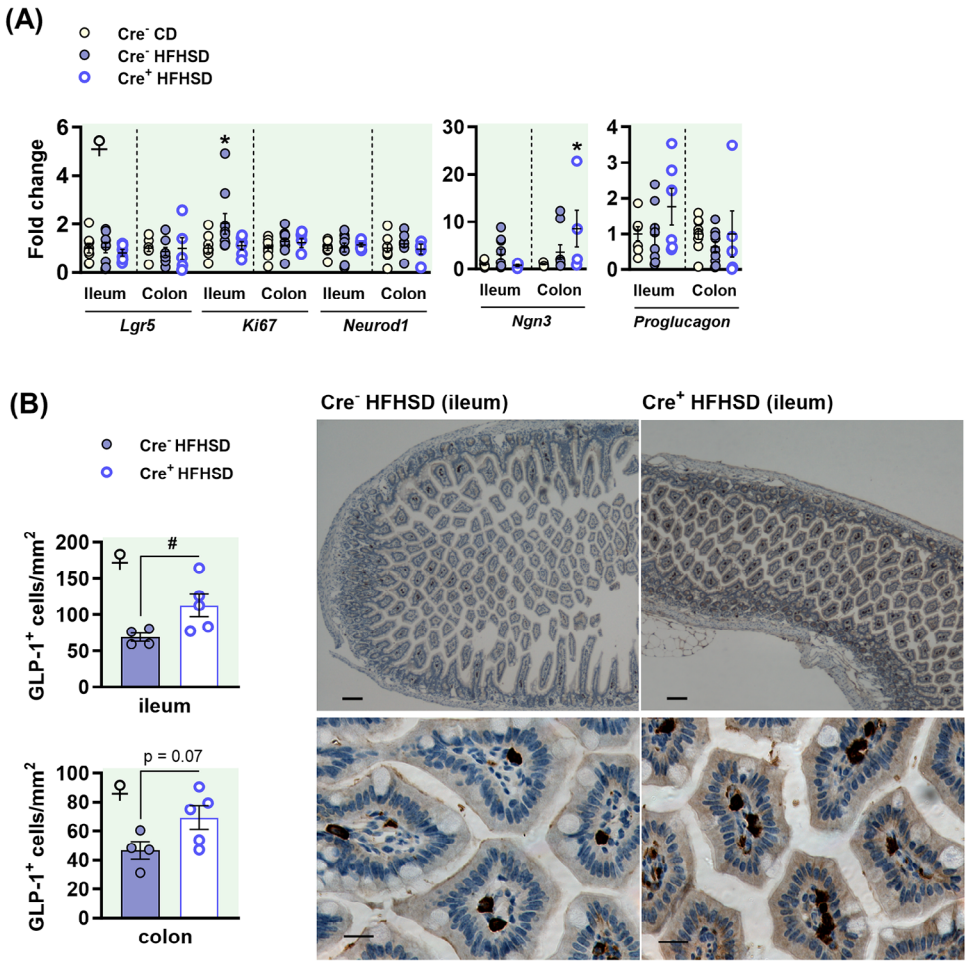

Figure 5. Deficiency of Nav1.8+ neurons increases the number of glucagon like peptide-1 (GLP-1)+ cells in the distal gut of female mice fed high-fat high-sugar diet. In female controls (Cre$^-$) fed control or high-fat high-sugar diet (CD or HFHSD, respectively) and mice lacking Nav1.8+ neurons (Cre$^+$) fed HFHSD we measured at the end of the experiment: A) Gene expression of markers of stem cells (*Lgr5*), proliferation (*Ki67*), enteroendocrine cell differentiation (neurogenic differentiation 1 [*Neurod1*] and neurogenin-3 [*Ngn3*]), and the GLP-1 precursor (*Proglucagon*) in ileum and colon. B) Quantification of GLP-1+ cells in ileum and colon. Data are shown as the mean ± standar error of the mean (SEM). In A, Cre$^-$ CD/HFHSD, $n = 8$–9 and Cre$^+$ HFHSD, $n = 6$. In B, Cre$^-$ HFHSD, $n = 4$ and Cre$^+$ HFHSD, $n = 5$. (A) One-way analysis of variance (ANOVA) followed by Tukey's post-hoc test or the Kruskal–Wallis test followed by Dunn's post-hoc test. (B) Student's *t*-test. $^*p < 0.05$ versus Cre$^-$ CD-fed mice. $^{\#}p < 0.05$ comparisons between Cre$^-$ and Cre$^+$ fed HFHSD. Scale bars: 100 and 20 µm.

the colonic expression of the neuroendocrine cell differentiation marker neurogenin-3 (*Ngn3)* as compared with control mice fed CD (**Figure 5**A) suggesting the attenuation of cellular proliferation under HFHSD-feeding and the enhancement of neuroendocrine cell differentiation. Quantification of cells expressing GLP-1 in the distal gut in HFHSD-fed mice revealed higher cellular density in the ileum of Nav1.8-cre/DTA mice than in control mice and a trend for a higher density in colon ($p = 0.07$) (Figure 5B).

2.4. Lack of Nav1.8-Expressing Neurons Leads to Faster Gastrointestinal Transit in High-Fat High-Sugar Diet-Fed Female Mice

We reasoned that the absence of Nav1.8+ neurons might also affect the intestinal efferent tone and/or the enteric nervous system (ENS), in turn modulating gut transit and the pool of dietary GLP-1 secretagogues in the distal gut.

Gene expression analysis of neural markers involved in gut motility (relaxation or contraction) revealed lower ileal levels of the noradrenaline and vasoactive intestinal peptide (VIP) receptors (adrenoceptor beta 2 [*Adrb2*] and VIP receptor 2 [*Vipr2*], respectively), involved in relaxation processes, in Nav1.8-cre/DTA mice than in control mice on HFHSD (**Figure 6**A), and higher expression of *Vipr2* in HFHSD-fed controls than in CD-fed controls. Transcripts of the glial cell marker glial fibrillary acidic protein (*Gfap*) were increased in HFHSD-fed groups irrespective of the genotype (Figure 6A). In colon, HFHSD-fed Nav1.8-cre/DTA mice had higher *Adrb2* mRNA levels than both control groups (CD and HFHSD), and increased gene expression of the metabotropic glutamate receptor 5 (*Grm5*), involved in contraction processes, compared with CD-fed controls (Figure 6B).

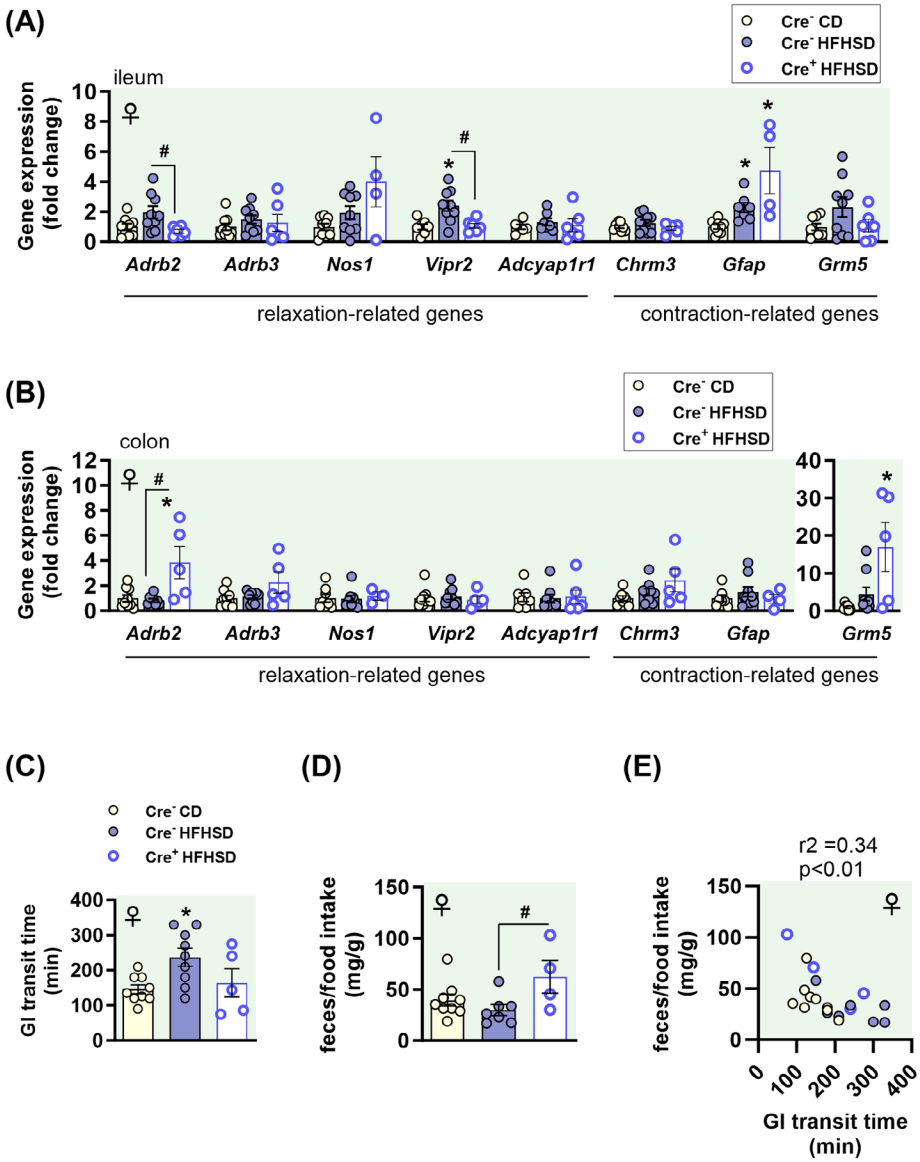

Figure 6. Deficiency of Nav1.8+ neurons alters the gene expression of gut motility-related neural markers and accelerates the gastrointestinal transit in female mice fed high-fat high-sugar diet. In female controls (Cre^-) fed control diet (CD) or high-fat high-sugar diet (HFHSD) and females lacking Nav1.8+ neurons (Cre^+) fed HFHSD, we measured: A, B) At the end of the experiment, the ileal and colonic mRNA levels of adrenergic receptors (*Adrb2* and *Adrb3*), nitric oxide synthase (*Nos1*), the receptor of vasoactive intetinal peptide (VIP) and pituitary adenylate cyclase-activating polypeptide (PACAP) (*Vipr2* and Adcyap1r1, respectively), the cholinergic receptor muscarinic 3 (*Chrm3*), the glial cell marker glial fibrillary acidic protein(*Gfap*) and the metabotropic glutamate receptor 5 (*Gmr5*). C) Time required for orally administered carmine red to appear in feces (gastrointestinal [GI] transit time) after 8 weeks of CD- or HFHSD-feeding. D) The production of feces in the carmine red trial normalized by the food intake. E) Correlation between the normalized feces production and the GI transit time. Data are represented as the mean ± standard error of the mean (SEM). Cre^- CD/HFHSD, $n = 8–9$; Cre^+ HFHSD, $n = 4–6$. One-way analysis of variance (ANOVA followed by Tukey's post-hoc test or the Kruskal–Wallis test followed by Dunn's post-hoc test. $^*p < 0.05$ versus Cre^- CD-fed mice. $^\#p < 0.05$ comparisons between Cre^- and Cre^+ fed HFHSD. ANOVA, analysis of variance; SEM, standard error of the mean.

Functional exploration of gut transit indicated that, compared with CD-fed control mice, HFHSD-feeding in controls, but not in Nav1.8-cre/DTA mice, increased the gastrointestinal transit time (Figure 6C) indicating a partial protection of the Nav1.8+ neurons ablation against the effect induced by the obesogenic diet. In addition, under HFHSD, the ablation of Nav1.8-expressing neurons increased the production of feces normalized by food intake (Figure 6D and Supporting Information Figure S4a,b), likely as a consequence of the partial restoration of the gastrointestinal transit time, as both variables showed a negative correlation (Figure 6E).

3. Discussion

Our data support a role for Nav1.8+ sensory neurons on the control of glucose homeostasis in female mice through a mechanism

originating in the gut that involves the upregulation of GLP-1 action.

Energy metabolism is differently regulated in females and males. For instance, fat depots show a sex-dependent distribution, with a preferential accumulation in visceral WAT in males, and in subcutaneous WAT in females,[26] as indicated by preclinical studies. This fat distribution confers protection against metabolic disturbances in females and increases the susceptibility in males, in line with the higher T2D prevalence in men.[27] Nevertheless, women, especially with menopause, are more prone to accumulate fat, leading to a higher prevalence of visceral obesity and metabolic syndrome than in men. [28] Despite these gender/sex-specificities, the development of strategies to improve metabolic health remains underexplored in females, even in preclinical models.

To provide mechanistic explanations of sex-related metabolic differences, we investigated further the recently identified function of Nav1.8+ neurons on energy balance[13–17] with an especial focus on gastrointestinal tract elements affecting energy metabolism.

Our study demonstrated sex-related influence of these neurons on body weight gain and glucose intolerance in mice on an obesogenic diet.

The relevance of Nav1.8+ neurons on the metabolic phenotype was already demonstrated in a recent work.[16] More specifically, the constitutive mTOR activation in Nav1.8+ neurons due to tuberous sclerosis complex 2 gene (*Tsc2*) knocking out in these neurons (Nav1.8-TSC2KO mice) modifies the distribution of adipose tissues in both female and male mice, promoting an obese phenotype, but prevents high fat diet-induced weight gain.[16] Our findings further support the role of Nav1.8-expressing neurons on energy metabolism. In particular, using Nav1.8+ neurons-deficient mice, we found that these neurons are dispensable for diet-induced obesity in females, but their absence induces resistance to gain weight in males. We identified that Nav1.8-cre/DTA male mice show diverse responses to HFHSD-feeding. The analysis of the body weight gain data in separated quartiles revealed that Nav1.8-cre/DTA male mice from the first quartile gained the same weight than their control littermates in response to HFHSD-feeding, which is in line with previous investigations.[15] In contrast, male mice from second, third and fourth quartiles gained less weight than their control littermates or even showed body weight loss relative to their initial weight. We also found that, while gonadal fat depots of Nav1.8-cre/DTA female mice were not affected, male mice lacking Nav1.8+ neurons that did not lose weight but showed resistance to obesity (Q2 and Q3) exhibited reduced gWAT with smaller adipocytes. Food intake does not seem to contribute to the resistance to obesity in Nav1.8-cre/DTA male mice. Indeed, loss of Nav1.8+ neurons did not affect ad libitum food intake and surprisingly exacerbated HFHSD refeeding after fasting, but with minimal weight gain. In this regard, the reduced food efficiency of Nav1.8-cre/DTA male mice fed HFHSD supports a low contribution of food as a source for weight gain in these mice. Defective cholesterol and fatty acid sensing in Nav1.8+ neurons exacerbates energy expenditure[29] which could also be the case of the total ablation of Nav1.8-expressing neurons, similarly contributing to attenuate fat storage under HFHSD. Complementary, our findings support that loss of Nav1.8+ neurons diminished lipid absorption after a meal in male mice, which could lead to reduce hypothalamic lipid sensing after a meal, explaining the exacerbated refeeding we have identified.

Importantly, the occasional weight loss we observed in Nav1.8-cre/DTA male mice fed HFHSD was associated with ulcerative dermatitis with skin lesions similar to those shown by Nav1.8-TSC2KO mice.[16] Although we did not perform behavioral analyses in Nav1.8-cre/DTA male mice, these skin lesions could be a consequence of an itch-related behavior as exhibited by Nav1.8-TSC2KO mice.[16] This sickness-related phenotype was only detected in males fed an obesogenic diet and finally caused death in our model. In agreement with other findings, these observations in Nav1.8-cre/DTA mice could reflect their inability to resolve the lesion-related inflammation due to defective immune response especially under high fat diet, as previously suggested.[15]

Since visceral fat is a main contributor to insulin resistance in obesity,[26] the reduced visceral (gonadal) fat observed in Nav1.8-cre/DTA male mice might favor glucose tolerance. We found sex-dependent effects of Nav1.8+ neurons on this variable. The improved glucose tolerance in male Nav1.8-cre/DTA mice was seen in response to intraperitoneal challenge with glucose, whereas oral glucose tolerance was enhanced in female Nav1.8-cre/DTA mice, suggesting a contribution of the intestinal Nav1.8+ afferents in the control of the postprandial whole-body glucose clearance in females but not in males.

There is evidence that supports improvements in glycemic control in people with obesity and T2D subjected to neuromodulation strategies such as VBLOC therapy.[30,31] Mechanistically, the inhibition of vagal afferents prevents the PPARα-mediated glucose intolerance induced by glucocorticoids,[32] although neither oral glucose tolerance nor sex-associated effects were explored in the aforementioned study. Our present findings demonstrate: (1) a postprandial glucoregulatory role of Nav1.8+ sensory neurons, occurring preferentially in females, (2) particularly those Nav1.8+ neurons innervating the gut, and (3) independently of confounding effects due to body weight variations.

Different explanations for the glucoregulatory effects of Nav1.8+ neurons in obese females are possible. Focusing in gastrointestinal mechanisms, on the one hand, the absence of Nav1.8+ neurons seemed to provide protection against systemic inflammation, as suggested by the effect of the neuronal ablation preventing splenomegaly, which could be a consequence of the anti-inflammatory tone of the intestine in Nav1.8-cre/DTA mice. Indeed, using the same mouse model, Talbot et al. demonstrated that the absence of Nav1.8+ neurons reduces the antigen-induced airway inflammation and bronchial hyperresponsiveness.[33] Nevertheless, further investigations are required to explore potential neuroimmune interactions between Nav1.8+ neurons and Treg and macrophages in the gut.

We also revealed changes in the enteroendocrine system which via endocrine routes can directly modulate glucose homeostasis in peripheral organs. The ablation of Nav1.8+ neurons impeded GIP oversecretion induced by HFHSD-feeding, which in turn may contribute to preventing the higher glucagon levels that accounts for the development of T2D.[34,35] The attenuated GIP oversecretion under an obesogenic diet in this mouse model may be a consequence of the accelerated gastrointestinal transit that in turn could reduce the availability of GIP secretagogues in the upper gut.[36]

On the other hand, the faster intestinal glucose uptake in Nav1.8-cre/DTA mice could lead to an earlier glucose sensing in pancreatic β-cells to induce insulin secretion. In addition, the depletion of Nav1.8+ neurons prevented the reduction of total GLP-1 levels induced by HFHSD-feeding seen in control mice, which could in turn improve pancreatic β-cell function and peripheral insulin sensitivity.[37] Altogether, these mechanisms may lead to the oversecretion of insulin observed in Nav1.8-cre/DTA mice independently of the prandial condition, allowing for a more efficient postprandial glucose clearance. Nonetheless, it cannot be ruled out that the insulin oversecretion without meal-related stimuli (i.e., fasting) might finally lead to long-term insulin resistance.

Analysis of the GLP-1 system in Nav1.8-cre/DTA mice revealed that the lack of Nav1.8+ neurons did not improve total GLP-1 secretion after 15 min of oral glucose or Ensure®, which corresponds to the early hormone release regulated by nutrient-mediated neural pathways.[38] By contrast, whatever the diet, postprandial total GLP-1 was higher in mice lacking Nav1.8+ neurons at 90 min after the oral Ensure®, corresponding to the later GLP-1 release directly driven by nutrients not absorbed in upper regions and reaching the distal gut.[38] In line with this, the accelerated gastrointestinal transit shown by female mice lacking Nav18+ neurons could contribute to increasing the availability of unabsorbed dietary GLP-1 secretagogues in distal intestinal regions, in turn favoring GLP-1 secretion and L-cell proliferation.

Since GLP-1 reduces gut motility and so increases gastrointestinal transit time,[39–41] we explored alternative mechanisms allowing a transit time reduction in female mice lacking Nav1.8+ neurons. The gene expression analysis of neural markers of the extrinsic and intrinsic nervous system involved in muscle contraction and relaxation in the intestine[42–46] revealed that the depletion of Nav1.8+ neurons upregulated muscle contraction markers and downregulated muscle relaxation markers, in line with the accelerated transit. Complementary, ENS changes due to the depletion of Nav1.8+ neurons may also have an impact on GLP-1, as the neuropeptides secreted by these neurons locally control GLP-1 release.[2]

Overall, the Nav1.8-cre/DTA phenotype in females resembles some of the metabolic benefits of bariatric surgery, including accelerated gastrointestinal transit, elevated levels in plasma of GLP-1 and insulin, and improved oral glucose tolerance.[5] These similarities suggest that, at least in part, the metabolic benefits of bariatric surgery could be a consequence of the loss of Nav1.8+ neurons. Indeed, it has been suggested that these benefits could be caused by the paradoxical increase of sensory inputs resulting from the unintentional vagotomy occurring during bariatric surgery,[47] in turn altering efferent visceral outflow and so, the physiology of the innervated organs.

Altogether, our study reveals sex-related differences in the function of Nav1.8+ afferent neurons, which might illuminate a path to personalized neuromodulation therapies that, through specific inhibition, could limit fat depots in overweight/obese men or improve postprandial glycemia in women with T2D. Notably, we describe that the improved postprandial glucose clearance in females due to ablation of Nav1.8+ afferents is aligned with intestinal adaptations leading to an amplified GLP-1 secretion and so, insulin secretion. These results open new possibilities for T2D treatment specifically in women based on non-invasive strategies by silencing Nav1.8-expressing neurons that mimic bariatric surgery effects.

Further studies are required to determine the spinal or vagal nature of the Nav1.8+ afferent neurons controlling energy homeostasis in a sex-dependent manner.

4. Experimental Section

Mice: Heterozygous Nav1.8 knock-in Cre-recombinase male mice (EM:04582, EMMA/Infrafrontier repository, Munich, Germany) were crossed with homozygous ROSA26-eGFP-DTA female mice (stock #006331; The Jackson Laboratory, Bar Harbor, ME) to obtain 1:1 L of Nav1.8-deficient mice (with Cre and DTA alleles: Nav1.8-cre/DTA or Cre^{+} in figures) and control mice (without Cre: control littermates or Cre^{-} in figures). Genotyping was conducted using the Phusion High-Fidelity PCR Kit (Thermo Fisher Scientific, Waltham, MA) (Supporting Information Table S1). RNA isolation and reverse-transcription were performed with the Ambion® RiboPure Kit (Invitrogen, Carsbad, CA) and SuperScript™ VILO™ Master Mix (Thermo Fisher Scientific), respectively, in randomly selected nodose ganglia. The TaqMan® PreAmp Master Mix (Applied Biosystems, Thermo Fisher Scientific) was used for cDNA pre-amplification, and TaqMan® Gene Expression Assays (FAM-MGB; Applied Biosystems) using TaqMan® Fast Advanced Master Mix (Applied Biosystems, Thermo Fisher Scientific) for gene expression analysis of *Scn10a* (coding for NAV1.8) and the housekeeping gene *Rpl19* (Supporting Information Table S1). Relative gene expression was calculated using the $2^{-\Delta\Delta Ct}$ method to represent data as fold-change relative to control littermates.

Experimental Design and Dietary Information: Three cohorts were generated for the experimental protocol detailed in Supporting Information Figure S1a. Collectively housed mice were maintained under constant conditions of humidity and temperature (23 ± 2 °C) and 12-h light/dark cycle with ad libitum access to food (and water) unless otherwise stated.

Female and male control and Nav1.8-cre/DTA mice (6 weeks old) were randomly allocated in groups fed either a CD (10% of energy from fat without sucrose) or an HFHSD (45% of energy from fat and 21% from sucrose) (D12450K or D12451, respectively, Research Diets) for 11 weeks. The composition of the diets is shown in Supporting Information Table S2.

Sample size (Supporting Information Figure S1a) was calculated using G*Power software based on a previously estimated effect size. Body weight was monitored weekly. Food efficiency, gastrointestinal transit time, and glucose tolerance were conducted in females and males between week 6 and 11. To estimate food efficiency (weight gain/food ingested during refeeding), mice were 4 h fasted in the dark phase followed by 2 h of free access to food. Gastrointestinal transit time was measured in overnight fasted mice receiving an oral gavage of 6% non-absorbable carmine red in 0.9% saline with 0.5% methylcellulose.[48] For 6 h, mice had free access to food and the color of feces was checked every 30 min to determine the time from the oral gavage to the first appearance of carmine red in feces. Feces after the overnight fasting and feces after the gastrointestinal transit time (6 h of refeeding) were collected to measure triglyceride levels. For glucose tolerance tests (GTTs), glycemia was determined at 0, 15, 30, 60, and 120 min after an oral (OGTT) or intraperitoneal (ipGTT) glucose challenge. At week 7, overnight-fasted male mice were ad libitum fed for 2 h to measured postprandial triglycerides in plasma.

Between week 7 and 11, intestinal glucose absorption and the glucose-induced hormone secretion (GLP-1, GIP, insulin, and glucagon) was explored in females. Intestinal glucose absorption was estimated by calculating the slope of the glycemia between 0 and 5 min after a glucose oral challenge,[49] and hormone secretion by measuring hormones in plasma at 0 and 15 min after an oral glucose load.

For GTTs, intestinal glucose absorption and hormone secretion, mice were fasted for 4 h before glucose challenge (2 g kg^{-1}). For the GTTs and glucose absorption, blood was drawn from the saphenous vein, and for hormone secretion tests, from the submandibular vein into Microvette®

500 K3E tubes containing DPPIV inhibitors (Sigma), and immediately centrifuged to obtain plasma. Glycemia was determined with Contour XT glucometer (Bayer, Leverkusen, Germany).

At the end of the experiment, 4 h fasted mice were orally administered the mixed nutrient solution Ensure® (12.4 kcal kg^{-1}) to assess GLP-1 levels at 0 and 15 or 90 min after Ensure® challenge. In one group of females, blood was collected 15 min after Ensure®, and mice were then sacrificed by cervical dislocation to isolate duodenum, ileum, colon, and brain, which were immediately frozen until processed. The remaining small intestine was embedded in cold FACS buffer for further isolation of immune cells. Another group of female and male mice were anaesthetized with an intraperitoneal injection of pentobarbital (50 mg kg^{-1}) 90-min following Ensure® administration, and were then transcardially perfused with PBS followed by 10% neutral buffered formalin. The gWAT and iWAT, respectively, of males and females and ileum and colon of females were isolated for processing.

Animal welfare was assessed on a daily basis. Signs of sickness or harm observed were immediately reported to the veterinarian in charge of the animal facility for further evaluation. Assessments were focused on excessive body weight loss, spine posture, dullness of mice coat and injury such as ulcerative dermatitis induced by self-mutilation. All the experimental procedures using animals, as well as evaluation of signs of sickness, were in accordance with European Union 2010/63/UE and Spanish RD53/2013 guidelines, and were approved by the ethics committee of the University of Valencia (SCSIE, UV, Spain) and authorized by Dirección General de Agricultura, Ganadería y Pesca (Generalitat Valenciana) (approval ID 2019/VSC/PEA/0020 and 2020/VSC/PEA/0022).

Hormone Levels in Plasma: GLP-1 (total), GIP, insulin, and glucagon in plasma were measured using a MMHE-44K-04 Milliplex Kit (Merck, Darmstadt, Germany) in a Luminex MAGPIX® System (Luminex, Austin, TX) or an ELISA kit for total GLP-1 (Merck).

Triglycerides in Plasma and Feces: Only in male mice, triglycerides levels were measured in feces after 12 h of overnight fasting and 6 h of refeeding, and in plasma after 2 h of refeeding. Lipids were isolated from feces based on a method adapted from refs. [50, 51] as previously described.[52] Triglycerides were measured using a Triglyceride Colorimentric Assay Kit (Elabscience Biotechnology Co. Ltd., Bethesda, MD).

Histology and GLP-1 Immunostaining: Hematoxylin-eosin staining was performed in gWAT and GLP-1 immunostaining in intestinal samples according to standardized protocols by Patologika Laboratorio S.L. (Valencia, Spain). Images were taken using an Eclipse 90i Nikon wide-field microscope (Nikon Corp., Tokyo, Japan) with a CFI Plan Fluor DIC M/N2 (MRH00200) Nikon dry-air objective (20× or 4×) combined with an optical zoom factor of 0.8×. Fiji software (ImageJ 1.49q Software, National Institutes of Health) and Nis elements BR 3.2 software (Nikon Corp.) were used for quantification according to standardized protocols of the imaging service from IATA-CSIC.

RT-qPCR: RNA was isolated from the hypothalamus, duodenum, ileum, and colon using TRIsure™ (Bioline Reagent, London, UK). Reverso-transcription and qPCR were performed as described.[53] Relative change of cDNA abundance was calculated according to the $2^{-(\Delta\Delta Ct)}$ method and represented as fold-change expression relative to the control group. Supporting Information Table S3 shows the specific primer pairs.

Immune Phenotyping by Flow Cytometry: Splenic suspensions, obtained by crushing and washing with FACS buffer (PBS-10% fetal bovine serum, Thermo Scientific), were filtered (70 µm nylon cell strainers, Biologix) and centrifuged (450 × *g*, 5 min, 4 °C). Intestines were incubated with Ca2+/Mg2+-supplemented Hank's balanced salt solution (HBSS) (Thermo Fisher Scientific) with 5 mM EDTA, 1 mM DTT, and antibiotics (100 µg mL^{-1} streptomycin–100 U mL^{-1} penicillin, Merck) for 30 min at 37 °C, filtered (100-µm nylon cell strainers, Biologix) and incubated again with HBSS containing antibiotics and 0.5 mgmL^{-1} collagenase D, 1 mg mL^{-1} DNase I (Roche), and 3 mg mL^{-1} dispase II (Sigma) for 30 min at 37 °C. Lamina propria cells were isolated by filtration (70-µm nylon cell strainers, Biologix) and centrifugation (450 × *g*, 5 min, 4 °C) of cell suspensions.

A combination of flow cytometry antibodies against surface and intracellular markers (Supporting Information Table S4) was used for immunolabeling FACS preserved cells (30 min at 4 °C, protected from light). Cells were first permeabilized and fixed using a fixation/permeabilization solution (BD Bioscience) for intracellular markers. Data acquisition and analysis were performed using a BD LSRFortessa flow cytometer operated with FACS Diva software v.7.0 (BD Biosciences).

Statistics: GraphPad Prism 9 was used for statistics. Normality and equality of variances were assessed with Shapiro–Wilk and Bartlett's tests, respectively. Two-way analysis of variances (ANOVAs) were used for main effects and interactions between genotype and diet, genotype and sex, or genotype and prandial conditions. Multiple comparisons using Tukey's post-hoc test were performed when interactions were detected. One-way ANOVA followed by Tukey's post-hoc test or Kruskal–Wallis followed by Dunn's post-hoc test were conducted for the analyses restricted to control mice fed either CD or HFHSD and Nav1.8-cre/DTA mice fed HFHSD. Matched pairs data were analyzed with paired *t*-tests and Student's *t*-test was used to explore differences between two independent groups. Correlations between two variables were explored with Bravais–Pearson correlation coefficient. Survival was analyzed using Log-rank (Mantel–Cox) Chi square test.

Supporting Information

Supporting Information is available from the Wiley Online Library or from the author.

Acknowledgements

The authors thank Inmaculada Noguera for excellent technical assistance and the animal technicians for animal care (SCSIE, University of Valencia), and to Dr. José María Coll Marqués (IATA-CSIC) for support in imaging procedures. This study received funding from the European Union Horizon 2020 research and innovation program under the Marie Sklodowska-Curie grant agreement No. 797297 (M.R.P.), the Spanish Ministry of Science and Innovation (Grant PID2020-119536RB-I00), the European Commission – NextGenerationEU, through the "CSIC Interdisciplinary Thematic Platform (PTI+) NEURO-AGING+" (PTI-NEURO-AGING+). The grant of the Spanish Ministry of Science and Innovation (MCIN/AEI) to IATA-CSIC as Accredited Center of Excellence (CEX2021-001189-S/MCIN/AEI/10.13039/501100011033) is acknowledged.

Conflict of Interest

The authors declare no competing interests.

Author Contributions

M.R.-P. and C.B.-V. contributed equally. M.R.P., C.V.B., and Y.S. designed the study. M.R.P. and C.B.V. conducted the in vivo experiments and M.R.P. supervised the research. C.B.V. conducted the sampling procedures. M.R.P. and C.B.V. analyzed the data. M.R.P. prepared figures and drafted the manuscript. Y.S. edited the manuscript and supervised the project.

Data Availability Statement

Data available on request from the corresponding author.

Keywords

glucagon like peptide-1 (GLP-1), Nav1.8+ sensory neurons, obesity, type 2 diabetes

Received: July 8, 2023
Revised: October 16, 2023
Published online: December 1, 2023

[1] P. Richards, N. A. Thornberry, S. Pinto, *Mol. Metab.* **2021**, *46*, 101175.
[2] A. Psichas, F. Reimann, F. M. Gribble, *J. Clin. Invest.* **2015**, *125*, 908.
[3] J. Karlsson, C. Taft, A. Rydén, L. Sjöström, M. Sullivan, *Int. J. Obes. (Lond.)* **2007**, *31*, 1248.
[4] P. R. Schauer, S. R. Kashyap, K. Wolski, S. A. Brethauer, J. P. Kirwan, C. E. Pothier, S. Thomas, B. Abood, S. E. Nissen, D. L. Bhatt, *N. Engl. J. Med.* **2012**, *366*, 1567.
[5] P. Larraufie, G. P. Roberts, A. K. McGavigan, R. G. Kay, J. Li, A. Leiter, A. Melvin, E. K. Biggs, P. Ravn, K. Davy, D. C. Hornigold, G. S. H. Yeo, R. H. Hardwick, F. Reimann, F. M. Gribble, *Cell Rep.* **2019**, *26*, 1399.
[6] R. E. Gimeno, D. A. Briere, R. J. Seeley, *Cell Metab.* **2020**, *31*, 679.
[7] C. Clemmensen, T. D. Müller, S. C. Woods, H.-R. Berthoud, R. J. Seeley, M. H. Tschöp, *Cell* **2017**, *168*, 758.
[8] M. A. Nauck, D. R. Quast, J. Wefers, J. J. Meier, *Mol. Metab.* **2021**, *46*, 101102.
[9] J. V. Pardo, S. A. Sheikh, M. A. Kuskowski, C. Surerus-Johnson, M. C. Hagen, J. T. Lee, B. R. Rittberg, D. E. Adson, *Int. J. Obes. (Lond.)* **2007**, *31*, 1756.
[10] M. Camilleri, *Gastroenterology* **2015**, *148*, 1219.
[11] C. M. Apovian, S. N. Shah, B. M. Wolfe, S. Ikramuddin, C. J. Miller, K. S. Tweden, C. J. Billington, S. A. Shikora, *Obes. Surg.* **2017**, *27*, 169.
[12] G. de Lartigue, *J. Physiol.* **2016**, *594*, 5791.
[13] J. Kupari, M. Häring, E. Agirre, G. Castelo-Branco, P. Ernfors, *Cell Rep.* **2019**, *27*, 2508.
[14] B. Abrahamsen, J. Zhao, C. O. Asante, C. M. Cendan, S. Marsh, J. P. Martinez-Barbera, M. A. Nassar, A. H. Dickenson, J. N. Wood, *Science* **2008**, *321*, 702.
[15] L. Gautron, I. Sakata, S. Udit, J. M. Zigman, J. N. Wood, J. K. Elmquist, *J. Comp. Neurol.* **2011**, *519*, 3085.
[16] H. K. Serlin, E. A. Fox, *J. Comp. Neurol.* **2020**, *528*, 816.
[17] S. Udit, M. Burton, J. M. Rutkowski, S. Lee, A. L. Bookout, P. E. Scherer, J. K. Elmquist, L. Gautron, *Mol. Metab.* **2017**, *6*, 1081.
[18] J. M. Brazill, D. Shin, K. Magee, A. Majumdar, I. R. Shen, V. Cavalli, E. L. Scheller, *Mol. Metab.* **2023**, *68*, 101664.
[19] K. L. Egerod, N. Petersen, P. N. Timshel, J. C. Rekling, Y. Wang, Q. Liu, T. W. Schwartz, L. Gautron, *Mol. Metab.* **2018**, *12*, 62.
[20] N. Dey, V. E. Wagner, L. V. Blanton, J. Cheng, L. Fontana, R. Haque, T. Ahmed, J. I. Gordon, *Cell* **2015**, *163*, 95.
[21] C. C. Schmitt, T. Aranias, T. Viel, D. Chateau, M. Le Gall, A.-J. Waligora-Dupriet, C. Melchior, O. Rouxel, N. Kapel, G. Gourcerol, B. Tavitian, A. Lehuen, E. Brot-Laroche, A. Leturque, P. Serradas, A. Grosfeld, *Mol. Metab.* **2017**, *6*, 61.
[22] L. H. Storlien, A. B. Jenkins, D. J. Chisholm, W. S. Pascoe, S. Khouri, E. W. Kraegen, *Diabetes* **1991**, *40*, 280.
[23] K. N. Frayn, P. F. Maycock, *J. Lipid Res.* **1980**, *21*, 139.
[24] I. López-Almela, M. Romaní-Pérez, C. Bullich-Vilarrubias, A. Benítez-Páez, E. M. Gómez Del Pulgar, R. Francés, G. Liebisch, Y. Sanz, *Gut Microbes* **2021**, *13*, 1.
[25] M. Romaní-Pérez, I. López-Almela, C. Bullich-Vilarrubias, L. Rueda-Ruzafa, E. M. Gómez Del Pulgar, A. Benítez-Páez, G. Liebisch, J. A. Lamas, Y. Sanz, *FASEB J.* **2021**, *35*, e21734.
[26] F. A. Duca, T. D. Swartz, Y. Sakar, M. Covasa, *Int. J. Obes. (Lond.)* **2013**, *37*, 375.
[27] B. E. Levin, *Obes. Res.* **1993**, *1*, 281.
[28] J.-Y. Choi, R. A. McGregor, E.-Y. Kwon, Y. J. Kim, Y. Han, J. H. Y. Park, K. W. Lee, S.-J. Kim, J. Kim, J. W. Yun, M.-S. Choi, *Int. J. Obes. (Lond.)* **2016**, *40*, 1452.
[29] S. Talbot, R.-E. E. Abdulnour, P. R. Burkett, S. Lee, S. J. F. Cronin, M. A. Pascal, C. Laedermann, S. L. Foster, J. V. Tran, N. Lai, I. M. Chiu, N. Ghasemlou, M. DiBiase, D. Roberson, C. Von Hehn, B. Agac, O. Haworth, H. Seki, J. M. Penninger, V. K. Kuchroo, B. P. Bean, B. D. Levy, C. J. Woolf, *Neuron* **2015**, *87*, 341.
[30] A. Jacobson, D. Yang, M. Vella, I. M. Chiu, *Mucosal Immunol.* **2021**, *14*, 555.
[31] D. A. Winer, H. Luck, S. Tsai, S. Winer, *Cell Metab.* **2016**, *23*, 413.
[32] E. Jeffery, A. Wing, B. Holtrup, Z. Sebo, J. L. Kaplan, R. Saavedra-Peña, C. D. Church, L. Colman, R. Berry, M. S. Rodeheffer, *Cell Metab.* **2016**, *24*, 142.
[33] B. Tramunt, S. Smati, N. Grandgeorge, F. Lenfant, J.-F. Arnal, A. Montagner, P. Gourdy, *Diabetologia* **2020**, *63*, 453.
[34] G. Pucci, R. Alcidi, L. Tap, F. Battista, F. Mattace-Raso, G. Schillaci, *Pharmacol. Res.* **2017**, *120*, 34.
[35] V. Mansuy-Aubert, L. Gautron, S. Lee, A. L. Bookout, C. Kusminski, K. Sun, Y. Zhang, P. E. Scherer, D. J. Mangelsdorf, J. K. Elmquist, *eLife* **2015**, *4*, e06667.
[36] S. Shikora, J. Toouli, M. F. Herrera, B. Kulseng, H. Zulewski, R. Brancatisano, L. Kow, J. P. Pantoja, G. Johnsen, A. Brancatisano, K. S. Tweden, M. B. Knudson, C. J. Billington, *J. Obes.* **2013**, *2013*, 1.
[37] S. A. Shikora, J. Toouli, M. F. Herrera, B. Kulseng, R. Brancatisano, L. Kow, J. P. Pantoja, G. Johnsen, A. Brancatisano, K. S. Tweden, M. B. Knudson, C. J. Billington, *Obes. Surg.* **2016**, *26*, 1021.
[38] C. Bernal-Mizrachi, L. Xiaozhong, L. Yin, R. H. Knutsen, M. J. Howard, J. J. A. Arends, P. Desantis, T. Coleman, C. F. Semenkovich, *Cell Metab.* **2007**, *5*, 91.
[39] S. Talbot, R.-E. E. Abdulnour, P. R. Burkett, S. Lee, S. J. F. Cronin, M. A. Pascal, C. Laedermann, S. L. Foster, J. V. Tran, N. Lai, I. M. Chiu, N. Ghasemlou, M. DiBiase, D. Roberson, C. Von Hehn, B. Agac, O. Haworth, H. Seki, J. M. Penninger, V. K. Kuchroo, B. P. Bean, B. D. Levy, C. J. Woolf, *Neuron* **2015**, *87*, 341.
[40] K. El, J. E. Campbell, *Peptides* **2020**, *125*, 170213.
[41] Y. H. Lee, M.-Y. Wang, X.-X. Yu, R. H. Unger, *Diabetologia* **2016**, *59*, 1372.
[42] K. Miyawaki, Y. Yamada, N. Ban, Y. Ihara, K. Tsukiyama, H. Zhou, S. Fujimoto, A. Oku, K. Tsuda, S. Toyokuni, H. Hiai, W. Mizunoya, T. Fushiki, J. J. Holst, M. Makino, A. Tashita, Y. Kobara, Y. Tsubamoto, T. Jinnouchi, T. Jomori, Y. Seino, *Nat. Med.* **2002**, *8*, 738.
[43] D. J. Drucker, *Cell Metab.* **2006**, *3*, 153.
[44] G. E. Lim, P. L. Brubaker, *Diabetes* **2006**, *55*, S70.
[45] S. S. Thazhath, C. S. Marathe, T. Wu, J. Chang, J. Khoo, P. Kuo, H. L. Checklin, M. J. Bound, R. S. Rigda, B. Crouch, K. L. Jones, M. Horowitz, C. K. Rayner, *Diabetes* **2016**, *65*, 269.
[46] T. Tolessa, M. Gutniak, J. J. Holst, S. Efendic, P. M. Hellström, *J. Clin. Invest.* **1998**, *102*, 764.
[47] A. Amato, L. Cinci, A. Rotondo, R. Serio, M. S. Faussone-Pellegrini, M. G. Vannucchi, F. Mulè, *Neurogastroenterol. Motil.* **2010**, *22*, 664.
[48] K. N. Browning, R. A. Travagli, *Compr. Physiol.* **2014**, *4*, 1339.
[49] A. M. Harrington, J. M. Hutson, B. R. Southwell, *Prog. Histochem. Cytochem.* **2010**, *44*, 173.
[50] N. J. Spencer, H. Hu, *Nat. Rev. Gastroenterol. Hepatol.* **2020**, *17*, 338.
[51] M. Costa, N. J. Spencer, S. J. H. Brookes, *Auton. Neurosci.* **2021**, *235*, 102854.
[52] A. J. L. Leembruggen, Y. Lu, H. Wang, V. Uzungil, T. Renoir, A. J. Hannan, L. A. Stamp, M. M. Hao, J. C. Bornstein, *Biomolecules* **2023**, *13*, 139.
[53] L. Gautron, *Front. Neurosci.* **2021**, *15*, 626085.